processes

MDPI

Article

Numerical Estimation of Gas Release and Dispersion from a Submarine Pipeline

Mingjun Yang *, Rui Jiang, Xinyuan Wu and Zhongzhi Hu

School of Mechanical Engineering, Sichuan University of Science and Engineering, Zigong 643099, China
* Correspondence: yangmingjun@suse.edu.cn

Abstract: Submarine pipeline gas releases and dispersions can cause safety concerns such as fire and explosion, which can cause serious casualties and property losses. There are many existing studies on the impacts of the horizontal diffusion distances of natural gas leakages from subsea pipelines, but there is a lack of research on the impact of influencing factors on vertical diffusion distances. Therefore, a diffusion model of natural gas leakage from a submarine pipeline is established by using the computational fluid dynamics method (CFD). The influence law and degrees of factors such as water depth at the leakage point, leak orifice size, leak pressure and the ocean current's velocity on the leakages and vertical diffusion distances of natural gases from submarine pipelines are systematically investigated. The results show that the leaked natural gas jet enters the sea water to form an air mass, which rises continuously under the action of the pressure in the pipe and the buoyancy of the sea water. The gas mass breaks into smaller bubbles affected by the interaction between the gas–liquid two phases and continues to float up and diffuse to the overflow surface. It is also found that the ocean current's velocity will affect the offset of leakage gas along the current direction; the depth of the leakage water, the pressure in the pipe and the leakage aperture will affect the time when the gas reaches the sea surface and the release area after a submarine pipeline's leakage. The research results would help to support risk assessments and response planning of potential subsea gas release accidents.

Keywords: submarine pipelines; gas release and dispersion; diffusion-influencing factors; VOF; risk assessment

Citation: Yang, M.; Jiang, R.; Wu, X.; Hu, Z. Numerical Estimation of Gas Release and Dispersion from a Submarine Pipeline. *Processes* **2023**, *11*, 1076. https://doi.org/10.3390/pr11041076

Academic Editors: Zhiqiang Huang, Mingjiang Shi, Gang Li, Zhen Chen and Yachao Ma

Received: 24 February 2023
Revised: 21 March 2023
Accepted: 28 March 2023
Published: 3 April 2023

1. Introduction

Driven by energy demand, oil and gas exploitation has gradually shifted from land to sea. In recent years, the exploitation of subsea oil and gas has gradually increased. Offshore oil production has been relatively stable since 2000, but the natural gas production of offshore oil fields has increased by more than 50% in the same period. The International Energy Agency has predicted that the offshore natural gas production will increase from 17.5 mboe/d to 29.6 mboe/d in the period 2016–2040 [1]. However, the potential risk of marine oil and gas leakage also increases gradually due to the complex and changeable marine environment and the increase of marine oil and gas production [2,3]. Submarine oil and gas leakage events occur from time to time all over the world. Once a subsea gas release happens, it will not only cause huge direct economic losses, but also pollute the surrounding marine environment, affect safe oilfield production and even cause casualties [4,5]. On 2 July 2021, a natural gas leakage accident occurred in the underwater pipeline connecting the drilling platform of Mexico National Oil Company in Campeche state of Yucatan Peninsula, resulting in a sudden fire on the sea about 150 m away from the platform [6]. According to the statistics of Fang et al., 184 submarine pipeline leakage accidents occurred in the Gulf of Mexico from 1967 to 2012, and 19 submarine pipeline leakage accidents were published and reported in China from 1998 to 2012 [4]. The accumulated submarine natural gas leaked and diffused to the sea surface may cause secondary malignant accidents such

as fires or explosions in cases of open fires, which poses a serious threat to the safety of offshore platforms, ships and personnel [5]. Thus, it is of great significance to study the leakages and diffusions of submarine natural gas pipelines.

Research on the leakages caused by submarine blowouts and pipeline failures has attracted extensive attention. The problem of submarine natural gas leakage mainly focuses on leakage detection [7–10]. In the process of submarine pipeline leakage and diffusion, there are many studies on oil leakage. Zhu and Yang studied the oil-spill process and influencing factors from submarine pipelines to free surface by using CFD simulations [11–13]. Jiang studied the oil diffusion from the submarine pipeline under water flow through a physical experiment [14]. Some scholars have also studied the diffusion law of CO_2 in the subsea [15,16]. After the natural gas leaks from the submarine pipeline, it diffuses in the seawater and forms a plume [17–20]. Wang et al. observed and quantified the flow behavior and fracture process of gas under a wide range of pore sizes and flows to predict the bubble sizes in submarine oil well blowouts and pipeline leakages [21]. Zhu et al. estimated the leakage rates of natural gas pipeline valves through the factor analysis and cluster analysis of acoustic emission signals [22]. Malik et al. studied the impact of natural gas release and diffusion and the resulting vapor cloud explosion on equipment damage and personnel deaths in complex multi-layer platforms [23]. Yapa presented the MEGADEEP model for simulating the transport of gas and hydrates released in deepwater [24]. Erik captured the free surface formed by surfacing bubble plumes by a volume of fluid model [25]. Zhao et al. developed a new formulation for gas–oil interactions with jets/plumes with the aim of understanding and quantifying the droplet formation from Deepwater Horizon blowout (DWH) [26]. Li et al. used CFD software to study the diffusion and deflagration of offshore gas generated by submarine gas release [27–29]. Li's underwater gas-dispersion simulations included the impact of a matrix of scenarios for different gas-release rates, water depths, ocean current speeds and leak positions on horizontal diffusion distances, but did not include leak size and pressure. Wu et al. developed a CFD model to describe the behavior of a subsea gas release and the subsequent rising gas plume [30]. Wu's article considers the effects of leakage aperture and water depth on horizontal diffusion distance.

The above research does not consider the entire process of natural gas diffusion from underwater to the water's surface and lacks research on the vertical diffusion distance of influencing factors. Aiming at the problem of natural gas diffusion caused by submarine gas pipeline leakages in typical shallow areas, the VOF (volume of fluid method) Euler multiphase flow model is used to research the laws and influencing factors of natural gas migration and diffusion under water. The entire process of natural gas leakage and diffusion from subsea pipelines to the sea's surface has been studied, as well as the effects of seawater depth, leak orifice size, leak pressure and ocean-current velocity on natural gas diffusion. This study has achieved a systematic understanding and effective evaluation of the risk of natural gas diffusion caused by submarine gas pipeline leakages in shallow sea areas. The research results provide reference for the risk management and prevention and control of submarine gas transmission pipelines in China.

2. Theoretical

2.1. Leakage Model

Submarine oil and gas pipelines are the lifeline of the development and transportation of marine oil and gas resources. Submarine pipelines will leak after being damaged by third-party damage, scouring and suspension, corrosion, natural disasters, human errors and other factors if the water depth exceeds the critical water depth they can bear. At this time, the average pressure in the pipe is greater than the ambient pressure outside the pipe. Assuming that the leakage port of the pipeline is circular, the instantaneous leakage rate of natural gas can be calculated by Equation (1) [31].

$$Q = C_D S p \sqrt{\frac{Mk}{ZRT}\left(\frac{2}{k+2}\right)^{k+1/k-1}} \quad (1)$$

$$V = \frac{Q}{3600S\rho} \tag{2}$$

$$S = \frac{\pi}{4}D^2 \tag{3}$$

where Q is the natural gas leakage rate, kg/h. C_D is the leakage coefficient, which is related to the shape of the crack, 1 for the circle, 0 for the triangle 95 and 0.9 for rectangle. Z is the natural gas compression factor. R is the gas constant, 8.314 J/(mol·K). k is the thermal insulation index of natural gas, 1.3. D is the leakage aperture of natural gas pipeline, mm. p is the absolute pressure of natural gas transmission, Pa. M is the molecular number of the natural gas mass, 0.017 kg/mol. T is the natural gas transmission temperature, K. V is the natural gas leakage rate, m/s. S is the leakage area of the natural gas pipeline, m^2. ρ is the natural gas density, kg/m^3.

2.2. Turbulence

The diffusion motion of leaked gas belongs to a complex, unsteady turbulent motion. Gas is sprayed out from the leakage port at a high rate in the case of natural gas leakage in a submarine gas transmission pipeline. The leakage velocity gradient and pressure gradient are very large. Therefore, the realizable k-e turbulence model is used to describe the turbulence characteristics of oil and gas movement so as to ensure the closure of the basic governing equations. The turbulent kinetic energy, Equation (4), and turbulent dissipation, Equation (5), are as follows [32,33]:

$$\frac{\partial(\rho k)}{\partial t} + \frac{\partial(\rho k u_i)}{\partial x_i} = \frac{\partial\left[\left(\mu + \frac{\mu_t}{\sigma_k}\right)\frac{\partial k}{\partial x_j}\right]}{\partial x_j} + G_k - \sigma\varepsilon \tag{4}$$

$$\frac{\partial(\rho k)}{\partial t} + \frac{\partial(\rho\varepsilon u_i)}{\partial x_i} = \frac{\partial\left[\left(\mu + \frac{\mu_t}{\sigma_\varepsilon}\right)\frac{\partial \varepsilon}{\partial x_j}\right]}{\partial x_j} + \rho C_1 E\varepsilon - \rho C_2 \frac{\varepsilon^2}{k + \sqrt{v\varepsilon}} \tag{5}$$

$$C_1 = \max\left(0.43, \frac{\eta}{\eta + 5}\right) \tag{6}$$

$$\eta = \left(2E_{ij}\cdot E_{ij}\right)^{1/2}\frac{k}{\varepsilon} \tag{7}$$

$$E_{ij} = \frac{1}{2}\left(\frac{\partial u_i}{\partial x_j} + \frac{\partial u_j}{\partial x_i}\right) \tag{8}$$

$$\mu_t = \rho C_\mu \frac{k^2}{\varepsilon} \tag{9}$$

$$C_\mu = \frac{1}{A_0 + A_s U^* K/\varepsilon} \tag{10}$$

$$A_s = \sqrt{6}\cos\varphi \tag{11}$$

$$\varphi = \frac{1}{3}\cos^{-1}\left(\sqrt{6}W\right) \tag{12}$$

$$W = \frac{E_{ij}E_{jk}E_{ki}}{\left(E_{ij}E_{ij}\right)^{1/2}} \tag{13}$$

$$U* = \sqrt{E_{ij}^2 + \widetilde{\Omega}_{ij}{}^2} \tag{14}$$

$$\widetilde{\Omega}_{ij} = \overline{\Omega}_{ij} - 3\varepsilon_{ijk}\omega_k \tag{15}$$

where σ_ε = 1.2, C_2 = 1.9 and A_0 = 4.0. G_k is the source phase generated by the gradient of the gas mass flow rate. σ_k is the Prandtl number of turbulent kinetic energy, σ_k = 1. ν is the kinematic viscosity, m^2/s. $\overline{\Omega}_{ij}$ is the time-averaged rotation-rate tensor observed in the reference frame with angular velocity ω_k. For the flow field without rotation, the second term in the calculation formula $U*$ is 0.

2.3. Free Surface Tracking Model

When natural gas leaks on the seabed, natural gas enters the sea water in the form of bubbles. These bubbles, with large initial momentum, rise in the seawater under the action of buoyancy, and finally form a floating plume jet under the interaction with the surrounding water environment [34,35]. The VOF model is used to simulate the leakage and diffusion of a pipeline because the VOF method can simulate the injection process of pipeline leakage, the rising process of bubbles in a liquid and track the steady-state and transient-state of the gas–liquid interface [36]. The VOF model tracks the fluid flow in each control body by constructing a fluid volume fraction function F and constructs the free-surface properties according to its function value and derivative value. The fluid volume fraction function F_q is defined as the ratio of the volume occupied by the q-phase to the total volume of the unit. If F_q = 1, it means that all in the unit are the q-phase fluid. If F_q = 0, it means that there is no phase-q fluid in the unit. If $0 < F_q < 1$, it indicates that the unit is an interface unit. F_q satisfies the following equation [37,38].

$$\frac{\partial F_q}{\partial t} + \frac{\partial (uF_q)}{\partial x} + \frac{\partial (vF_q)}{\partial y} = 0 \tag{16}$$

$$\sum_{q=1}^{2} F_q = 1 \tag{17}$$

where q is the fluid phase and u and v are the velocity of the fluid flowing in the X and Y directions, m/s, respectively.

3. CFD Calculation

In this work, the ANSYS 12.0 Fluent was selected as the CFD simulation package. To ensure accurate calculation of the convection and diffusion terms, the second order upwind scheme and the second order central difference scheme are used, respectively. For convective terms, second-order upwind scheme is selected. The second-order central-differencing scheme is used for diffusion terms calculation. The convergent criteria for all calculations are set as that the residual in the control volume for each equation is smaller than 10^{-5}.

3.1. Physical Model and Mesh

Wilkening et al. found that the calculation results of the two-dimensional simulation model had good similarity with the three-dimensional model [39]. In addition, considering CPU consumption and calculation time, a two-dimensional model was established to simulate the process of gas leakage. In this paper, a leakage pipeline with a seawater depth of 50 m was studied, and the transverse research area was 50 m; that is, the study area was a square area of 50 m × 50 m (Figure 1). The leakage aperture was set at 50 m away from the horizontal plane, considering the influence of ocean current. The physical models were established for the leakage apertures of 0.02 m, 0.05 m and 0.1 m, respectively. The coordinates at the leakage hole were defined as (0, 0); that is, the x-axis coordinate range of the study area was $-25 \leq x \leq 25$ and the y-axis coordinate range was $0 \leq y \leq 50$.

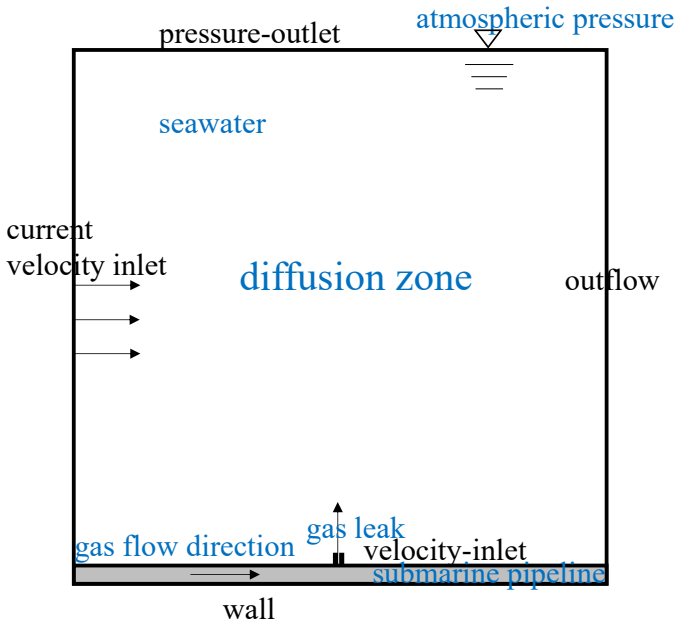

Figure 1. Calculation area and boundary conditions.

The calculation grid of the numerical model adopted a non-uniform grid, and the model was meshed by ICEM CFD (Figure 2). When the natural gas of a submarine pipeline leaks, a large amount of natural gas around the leakage point will enter the sea water, which will produce a violent flow. Therefore, the grid at the natural gas leakage port of submarine pipeline was densified. The number of grids has a significant influence on the simulation's efficiency and accuracy. A mesh sensitivity study was carried out prior to the analysis to ensure that the results obtained using the chosen grid achieved grid independence. The EquiSize Skew of 99.3% grids was between 0 and 0.4 when the number of grid cells was 1146971, which indicated that the grids had excellent quality.

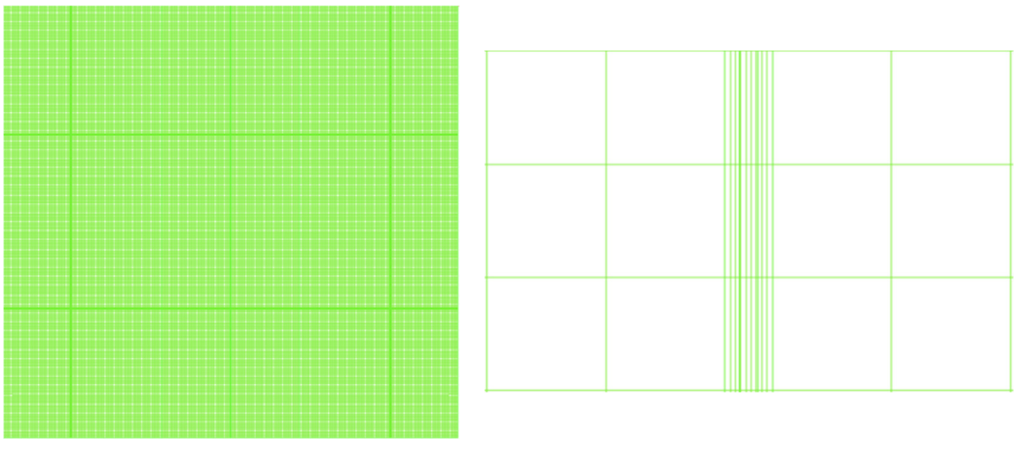

(**a**) (**b**)

Figure 2. (**a**). Mesh generation for modelling pipeline leakage. (**b**). Partial enlarged view of leakage orifice.

3.2. Boundary Conditions

The boundary conditions of the simulation model were set as shown in Figure 1. The leaking pipe was located at the bottom of the calculation area, where it was set as the wall. The leakage port of the pipeline was set as the gas-velocity inlet and the value was calculated by Formulas (1)–(3). The left side of the calculation area was the ocean-current inlet and the right side was the ocean-current free-outflow boundary. The ocean current direction

was horizontal to the right. The top of the calculation area was a free-liquid surface and the boundary condition was set as the pressure outlet. The value was 0 Pa, indicating that the gas pressure was the standard atmospheric pressure (relative pressure is 0).

It was assumed that the leakage point of natural gas in the submarine pipeline was 50 m below the sea surface. The nominal diameter of the pipe was 618 mm, and the wall thickness of the pipe was 20 mm. The length of the pipe was 50 m for research. The sea water density ρ_{water} = 1025 kg/m^3 and the viscosity μ_{water} = 0.00175 kg/m·s. It was assumed that the natural gas composition was an ideal CH_4 with a temperature T = 290.15 k. The diameter of the leakage orifice D = 100 mm and the pressure p = 5 MPa (absolute pressure) at the leakage point. The leakage flow rate of natural gas v = 267.9 m/s according to Equations (1)–(3).

The material properties were defined as methane gas in the gas phase and seawater in the liquid phase in the process of simulation.

3.3. Model Validation

The CFD simulation used in this study was validated against the numerical simulations reported in Li et al. (2018) [28], which also employed the VOF model in ANSYS. Four sets of numerical simulations were performed using the ocean current velocities of 0.5 m/s, 0.6 m/s, 0.7 m/s and 0.8 m/s. The horizontal dispersion distances were computed and compared, as shown in Figure 3. The obtained results demonstrate good agreement with the published CFD simulation results.

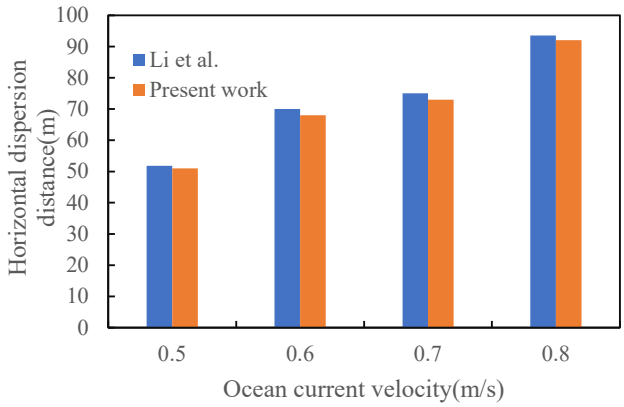

Figure 3. Validation of numerical simulation model against simulation results in Li et al. (2018) [28].

4. Results and Discussion

4.1. Subsea Gas Release and Dispersion

Figure 4 shows the whole process of gas release and dispersion from a submarine pipeline, in which the blue area is replaced by seawater, the red area is the leaked natural gas and different colors represent different gas–liquid volume fractions. The simulation results of gas leakage and diffusion in a submarine pipeline show that the gas diffusion and leakage process can be roughly divided into three stages.

First Stage: The leaked natural gas is given a higher initial momentum due to the pressure in the natural gas pipeline and enters the seawater at a higher initial speed at the initial time of leakage. The natural gas forms a small gas mass at the leakage orifice. The natural gas is attached to the outer wall of the submarine pipeline under the action of surface tension and grows laterally along the outer wall, so that the width of the gas mass is much larger than the diameter of the leakage orifice.

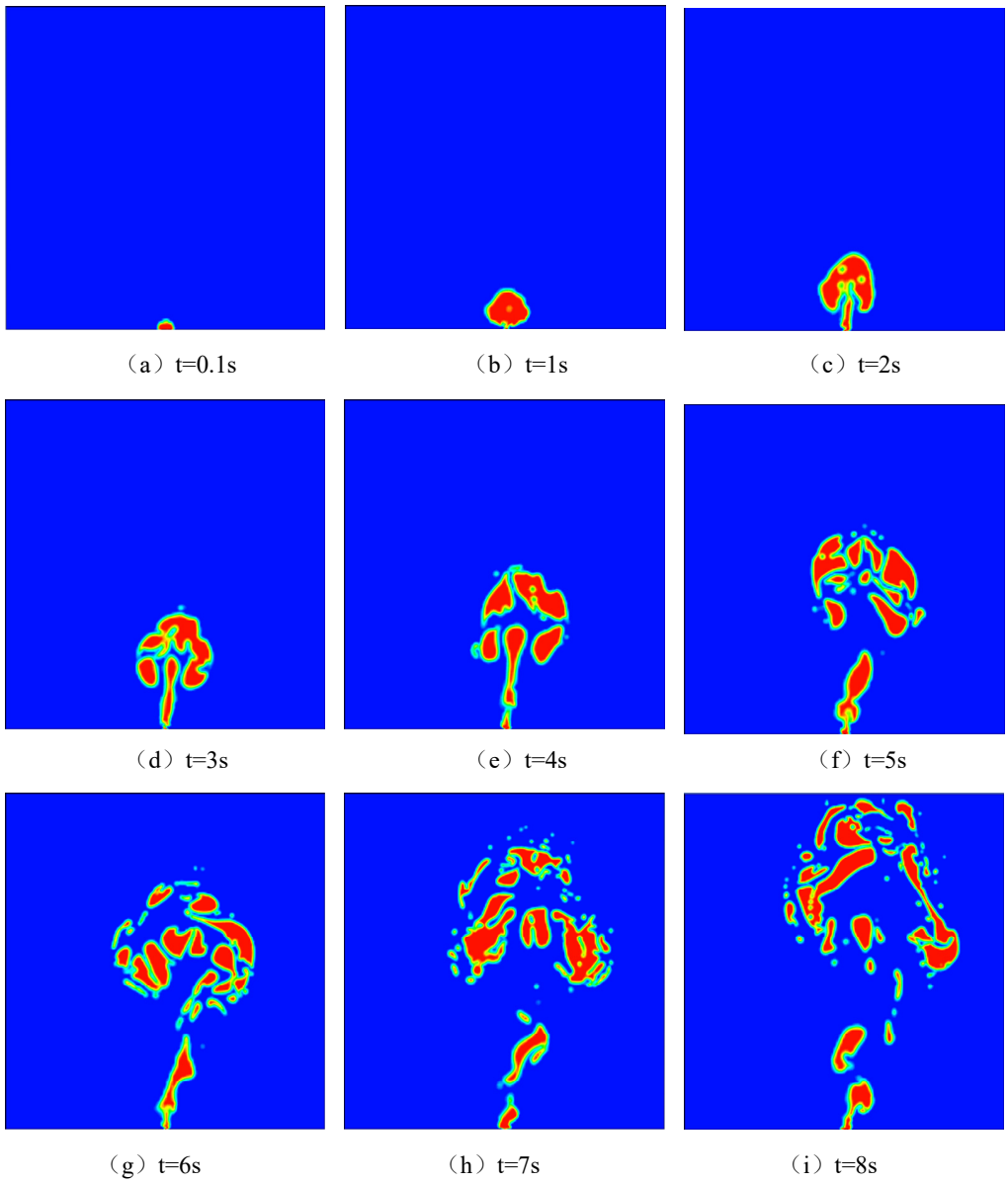

Figure 4. The whole process of gas release and dispersion from a submarine pipeline leak.

Second Stage: The gas mass rises gradually under the action of the initial momentum given by the pressure in the pipe and the buoyancy of sea water. The initial kinetic energy of the gas mass begins to decrease gradually after being injected into the sea water. The rising speed of the gas mass is slowed down by the resistance of the sea water during the rising process. However, gas continuously enters the seawater from the leakage port for replenishment during the rising process of the gas mass, making its rising speed relatively fast and continuously moving in the seawater to form a vortex state. The gas mass gradually forms a mushroom shape in the seawater.

Third Stage: The gas mass rises continuously with the increase of time under the action of seawater buoyancy. Its shape changes irregularly, gradually breaking and dispersing into multiple small bubbles due to the interaction of surface tension, buoyancy, inertia force and other forces between the gas and liquid. At the same time, the continuous upward floating and lateral movement make the distance of these small bubbles increase.

The flow rate of natural gas at the leakage port is high because of the large pressure in the submarine natural gas pipeline. Moreover, the density difference between the leaked natural gas and sea water in the pipeline is large (the density of natural gas is about

0.6679 kg/m^3 and the density of sea water is 1020~1025 kg/m^3), resulting in the leaked natural gas overflowing the water surface and diffusing into the atmosphere about 8 s after the leakage.

4.2. Analysis of Diffusion-Influencing Factors

4.2.1. Seawater Depth

The seawater flow rate (0 m/s), leakage aperture (100 mm) and pipeline pressure (5 MPa) were set as the fixed values. The water depths of 25 m, 50 m and 100 m were selected for numerical simulation to study the influence of seawater depth on the diffusion law of natural gas. Figure 5 shows the contours of gas volume fraction distribution at different times and at different water depths. From left to right, each figure shows the leakage and diffusion cloud map of natural gas at each time when the seawater depth is 25 m, 50 m and 100 m.

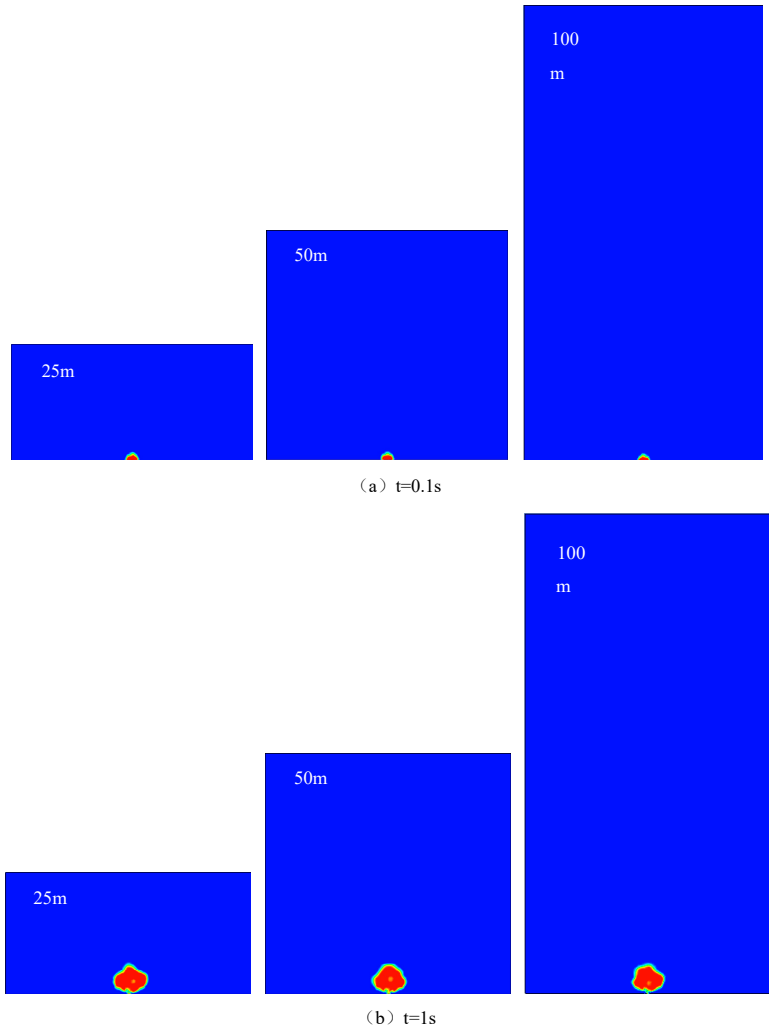

Figure 5. *Cont.*

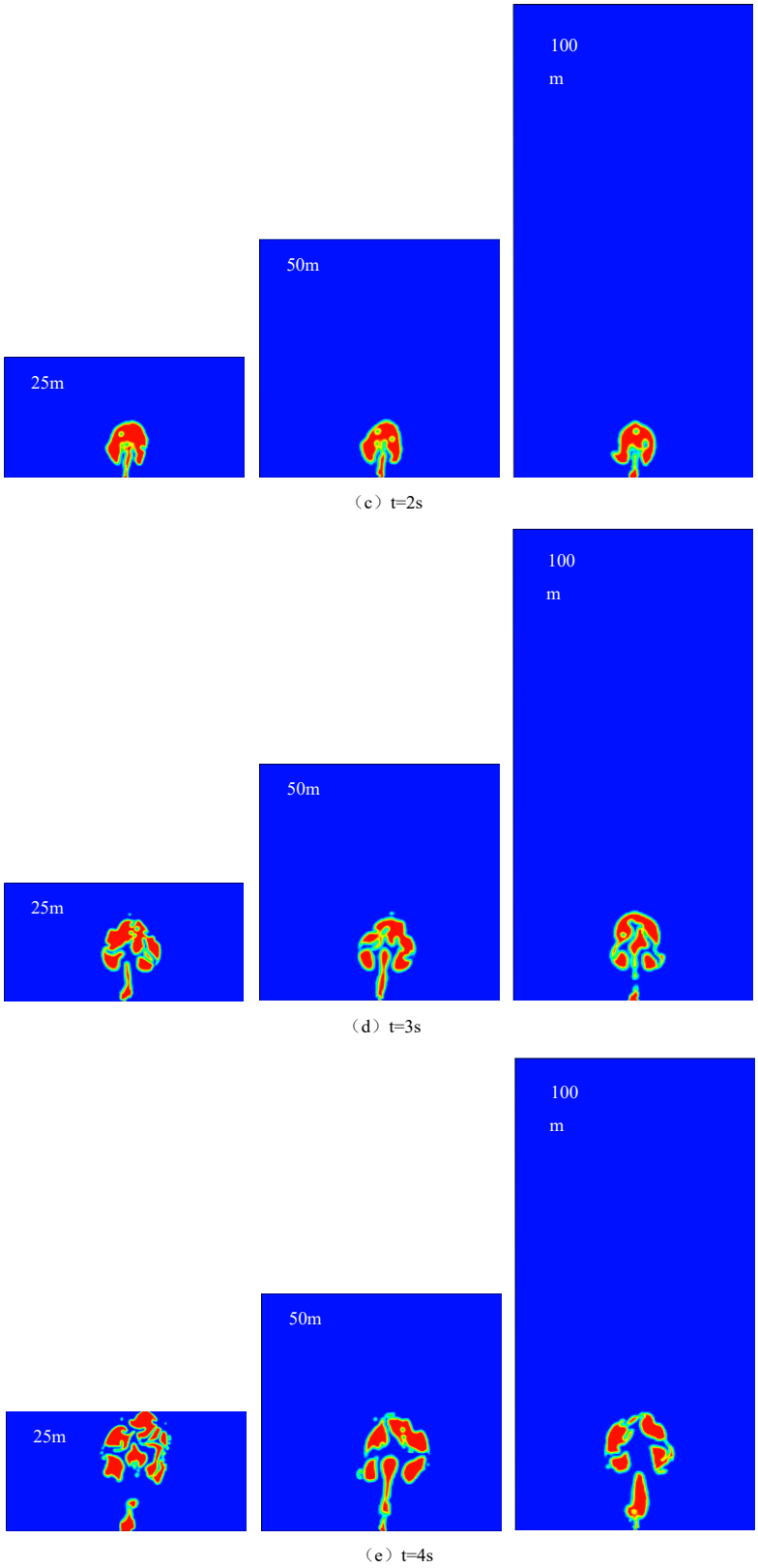

Figure 5. Cloud chart of submarine gas leakage and diffusion at each time when the water depth is 25 m, 50 m and 100 m, respectively.

As can be observed in the contours of natural gas volume fraction distribution in different water depths, the water depth will affect the transverse diffusion width of the leakage gas in the seawater. The diffusion width in the horizontal direction decreases with

the increase of water depth, which is more obvious in Figure 5e. In addition, the depth of the leakage point mainly affects the time of gas floating in the seawater. When the seawater depth is 25 m, the time of natural gas rising and diffusing to the sea surface is 4 s. When the seawater depth is 50 m, the time is 7.8 s. When the seawater depth is 100 m, the time is 11.9 s.

In summary, the influence of seawater depth on natural gas diffusion leakage is mainly reflected in two aspects: the width of the diffusion surface and the time to reach the sea's surface. For the leaked gas at the same location, the horizontal diffusion diameter increases with the decrease of water depth, and the time required for diffusion to the water surface decreases with the increase of water depth. The seawater depth of the leakage hole is the main factor affecting the floating and diffusion times of natural gas in seawater.

4.2.2. Leak Orifice Size

The water depth was set to 50 m, the seawater flow rate was set to 0 m/s and the pipeline pressure was set to 5 MPa to study the influence of the diameter of the leakage port on the natural gas leakage and diffusion law of the submarine pipeline. The natural gas diffusion patterns at different times of three different leak sizes, i.e., 20 mm, 50 mm and 100 mm, are illustrated in Figure 6.

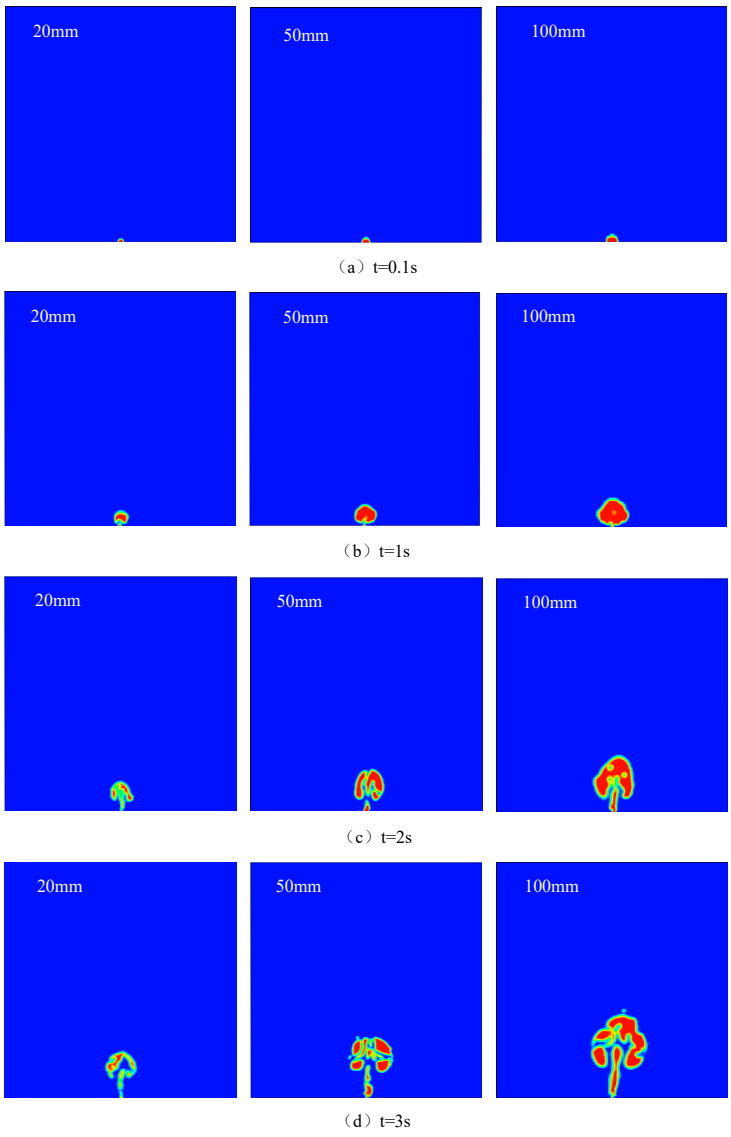

Figure 6. *Cont.*

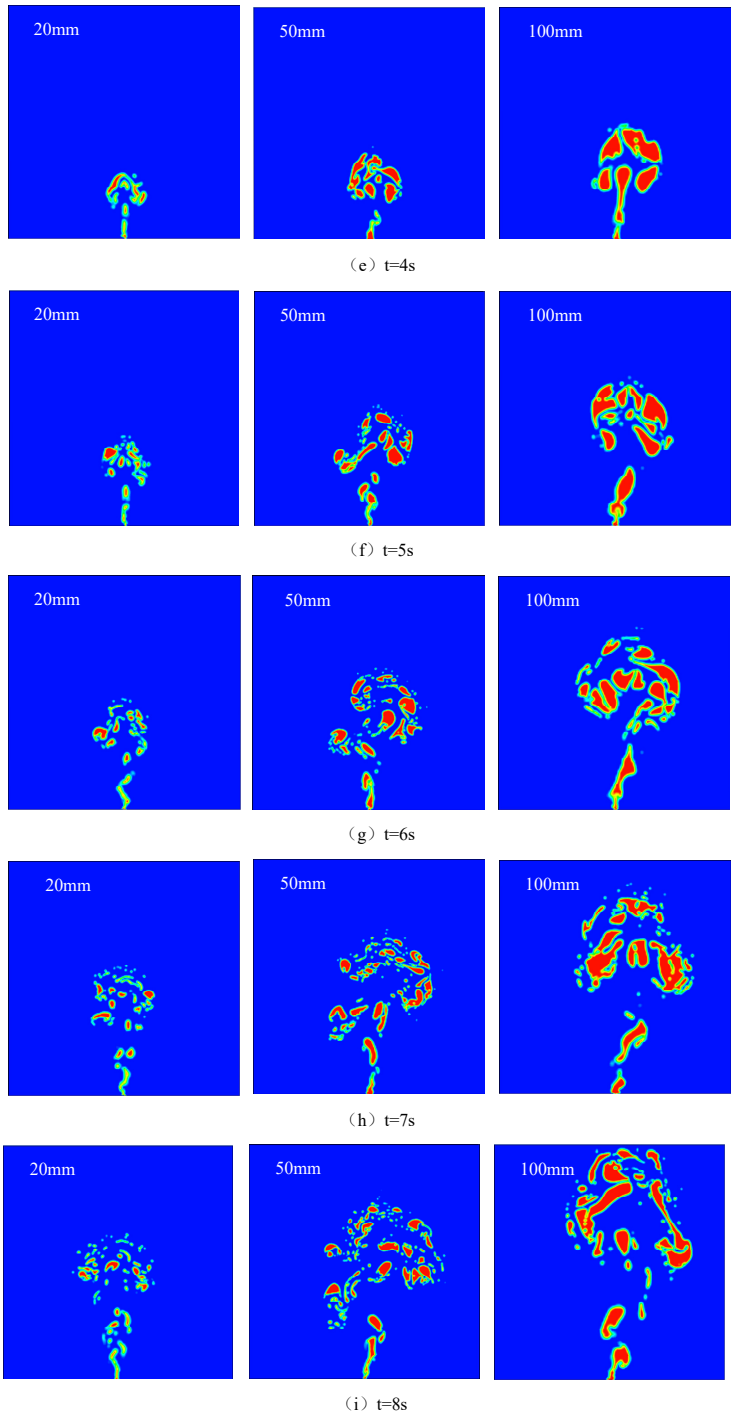

Figure 6. Leakage and diffusion nephogram of submarine natural gas at each time when the leakage aperture is 20 mm, 50 mm and 100 mm respectively.

Figure 6 shows that natural gas rises vertically in seawater without the influence of ocean currents. During the rising process, bubbles gradually break and diffuse in a relatively symmetrical state. When comparing the gas volume fraction distribution of the leakage and diffusion of submarine pipelines with different leakage diameters at the same time, it can be seen that the leakage amount and leakage trajectory of natural gas in seawater obviously vary with the leakage diameter. The size of the leakage diameter not only affects the amount of gas leakage and the leakage trajectory, but also affects the gas mass size and leakage rate. The gas mass size and gas leakage rate generated in seawater during the initial leakage increase with the increase of the leakage diameter. By comparing the gas

masses generated by different leakage apertures at the time of 3~8 s, it was found that the larger the diameters of the bubbles formed when natural gas masses are crushed by the interaction between the gas and liquid phases in seawater, the wider the range of diffusion to the water surface. The gas masses generated by large apertures rise faster. At 8 s, the gas masses with an aperture of 100 mm have already arrived at the sea surface, while the gas masses with apertures of 20 mm and 50 mm are still some distance from that. Therefore, attention should be paid to the protection of gas transmission pipelines in seawater, so as to prevent accidents such as explosion caused by large gas leakages due to a large aperture of a leakage port and to reduce economic losses and harm to the environment.

4.2.3. Leak Pressure

Setting the water depth (50 m), leakage aperture (100 mm) and seawater flow rate (0 m/s) as fixed values and selecting the pipeline pressures of 3 MPa, 5 MPa and 7 MPa, respectively, allows for a numerical simulation to study the influence of the pressure in the pipeline on the law of natural gas leakage and diffusion. Figure 7 presents the comparison of natural gas diffusion patterns with different pressures in the pipe with the increase of time.

The power of leakage mainly comes from the pressure in the gas-transmission pipeline in the initial stage of natural gas leakage. The initial rate of leaked gas varies when the pressure in the pipeline is different. The greater the pressure in the pipe, the greater the pressure difference with the surrounding environment. The pressure difference has a great influence on the leakage rate of the pipeline. A large pressure difference produces a faster leakage rate and more mass flow. The cloud diagram of gas volume fraction distribution under different pipe pressures at the same time shows that the faster and larger gas masses come from greater pressure in the tube. Especially after the leakage time reaches 3 s, it can be clearly seen that the gas mass generated by 7 MPa in the pipe is significantly greater than that generated by 3 MPa in the pipe. The gas-mass diagram at 8s shows that the gas mass generated by 7 MPa has reached the sea surface, while those generated by 5 MPa and 3 MPa are still some distance away from the sea surface. This indicates that the gas mass generated in the high-pressure pipeline rises faster under the greater buoyancy, and the shorter the time required for diffusion to reach the water surface.

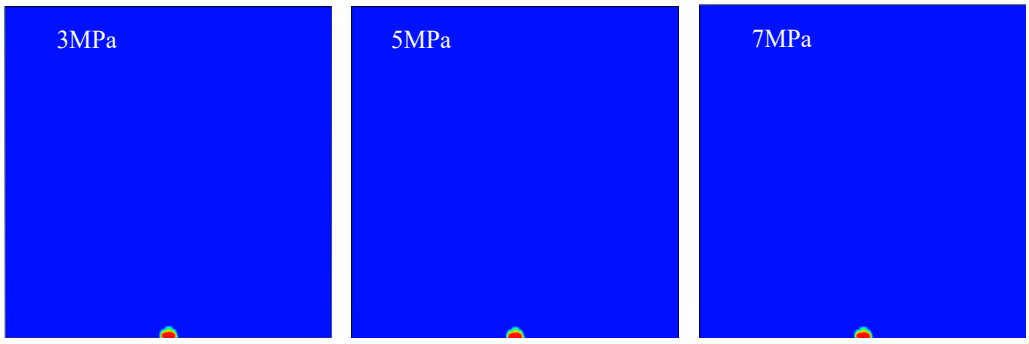

（a）t=0.1s

Figure 7. *Cont.*

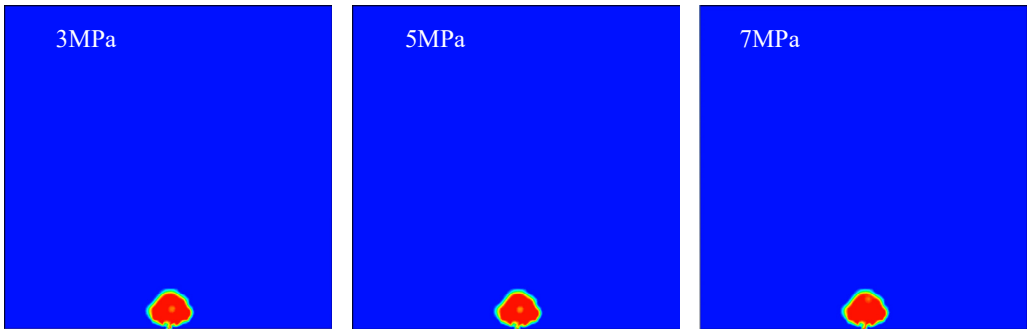

（b）t=1s

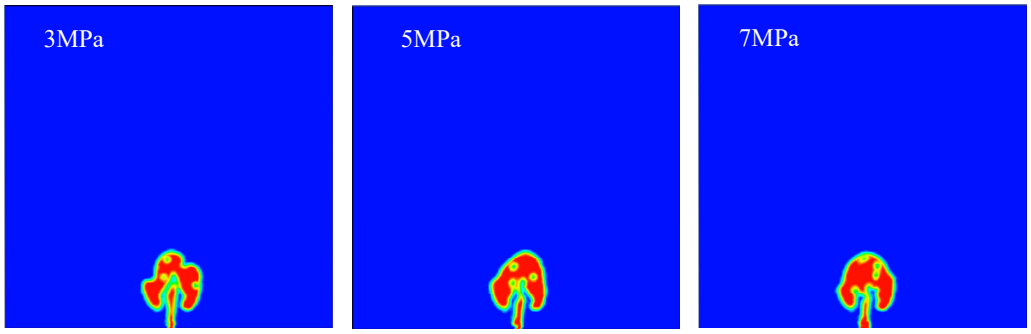

（c）t=2s

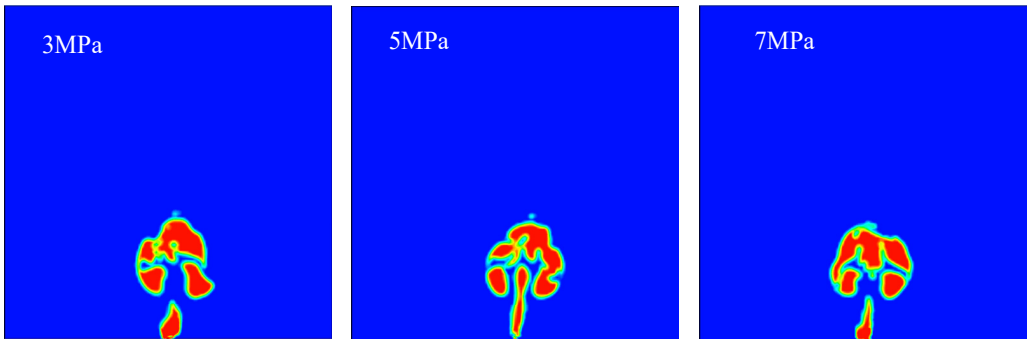

（d）t=3s

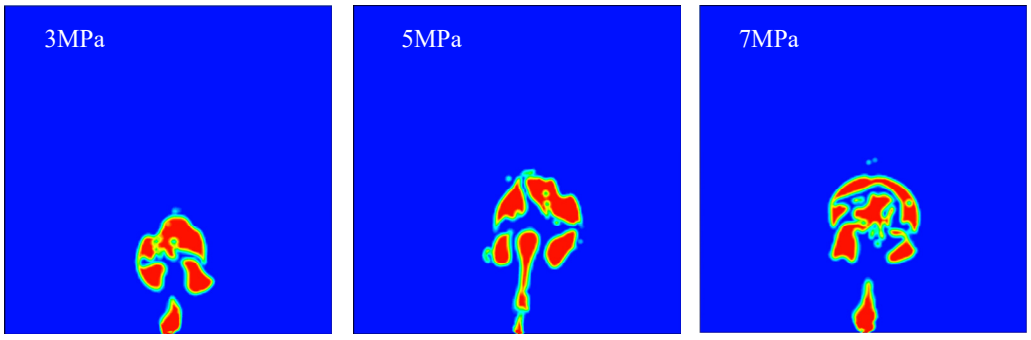

（e）t=4s

Figure 7. *Cont.*

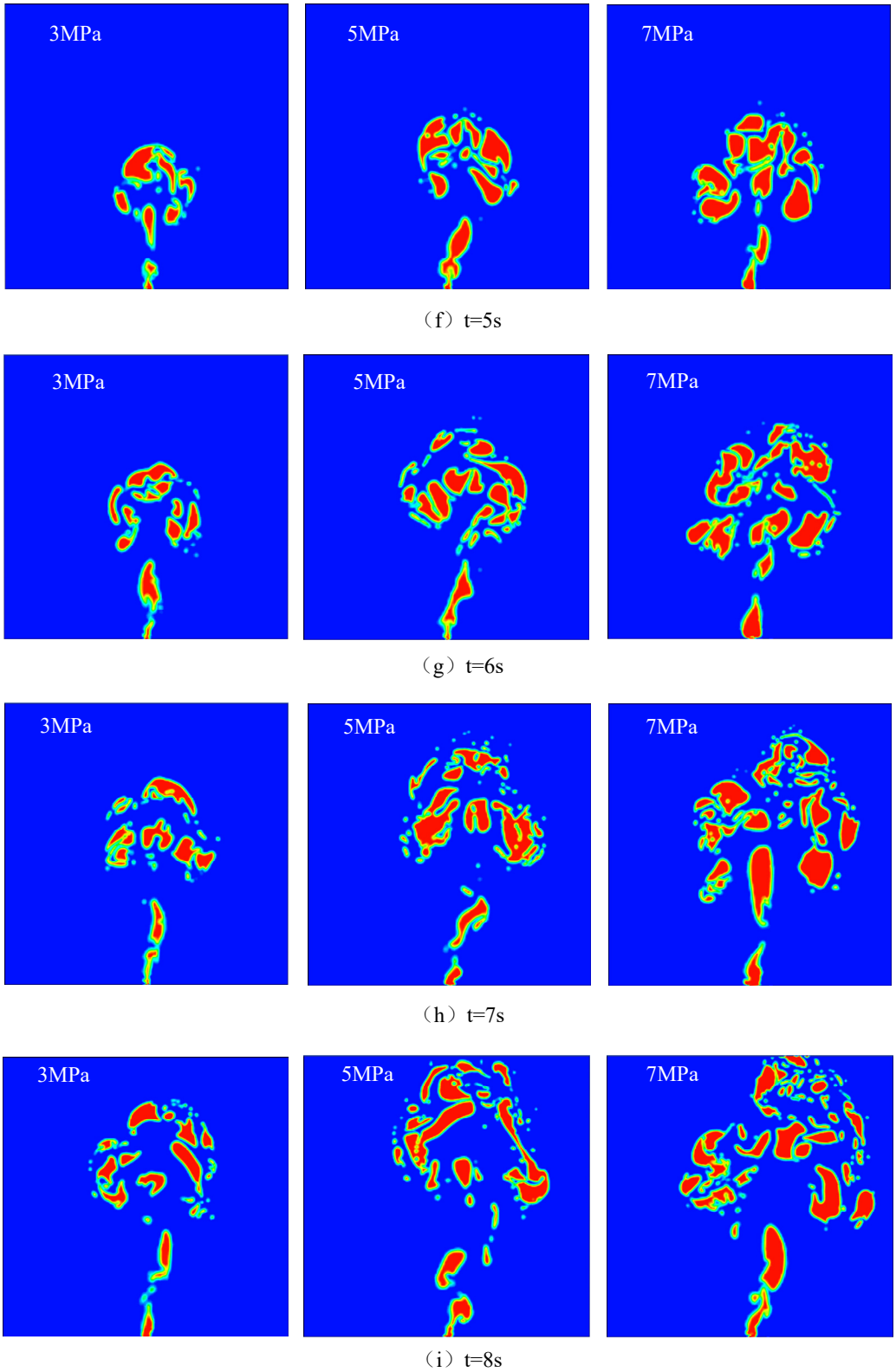

Figure 7. Nephogram of natural gas leakage and diffusion of submarine pipeline at each time when the pressures in the pipeline are 3 MPa, 5 MPa and 7 MPa, respectively.

4.2.4. Ocean Current Velocity

The movement after gas leakage is basically symmetrically distributed under the hydrostatic condition of uniform medium. There are some differences in seawater density due to the uneven distribution of algae, salt, sediment and other impurities in the marine

environment. There are also waves, ocean currents and other water movements in the marine environment, which have a certain impact on the leakage results. In particular, the ocean current's movement will cause the large lateral displacement of the leakage gas. The leakage gas will produce the maximum displacement and the leakage-diffusion radius reaches the extreme value along the direction of seawater movement [40].

Setting the water depth (50 m), leakage aperture (100 mm) and pipeline pressure (5 MPa) as fixed values and selecting the ocean current's velocity as 0 m/s, 0.4 m/s or 0.8 m/s allows for the numerical simulation to study the influence of the ocean current's velocity on the diffusion and leakage law of natural gas. The simulation results of the influence of the ocean current's velocity on the diffusion form of natural gas are shown in Figure 8.

Ny comparing the gas-mass cloud images and seawater flow rates of 0.4 m/s and 0.8 m/s with that of seawater at rest, it is found that the leaked gas will move towards the water flow direction due to the action of seawater flow when the seawater flow rate is not 0. Especially when the gas mass rises to a certain height and loses its initial momentum, the water flow velocity has a great influence on the offset of the leaked natural gas along the seawater flow direction. The larger the current velocity results, the farther the area that diffuses to the overflow surface is offset. In addition, the 2.5~4 s cloud diagram of gas masses at different seawater velocities shows that the smaller the seawater velocity, the faster the gas masses rise. This indicates that the water velocity will slow down the rate of gas rise. By comparing the cloud images of gas masses at the same time in Figure 8, it is also found that gas masses are relatively less affected by ocean currents due to the high initial kinetic energy, and changes in ocean current velocity have no significant impact on the diffusion pattern of natural gas.

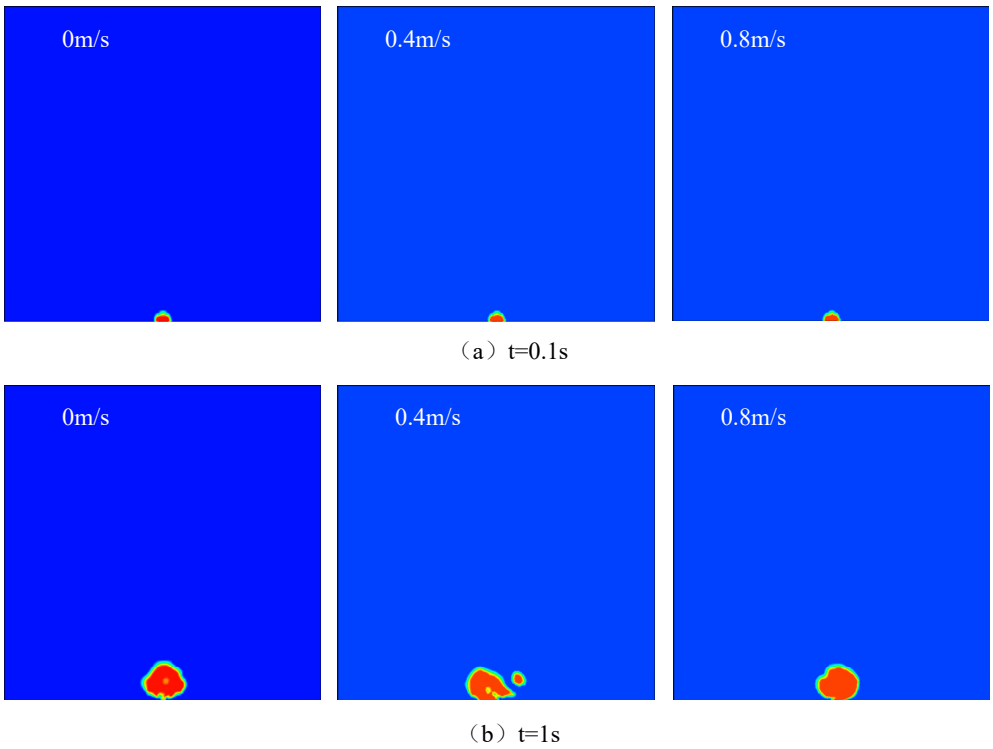

Figure 8. *Cont.*

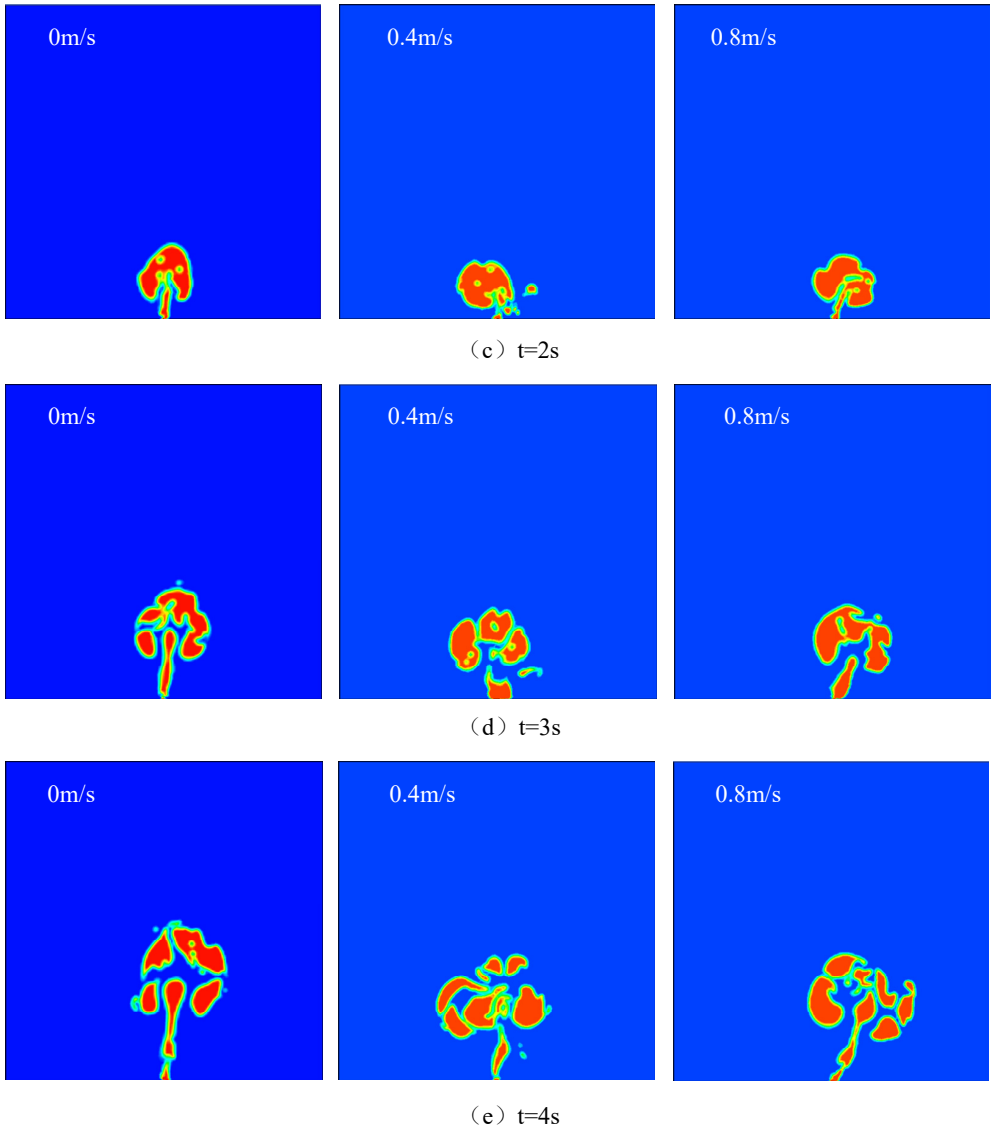

Figure 8. Cloud chart of natural gas leakage and diffusion of submarine pipeline at each time when the current velocity is 0 m/s, 0.4 m/s or 0.8 m/s, respectively.

5. Summary and Conclusions

The leakage of subsea pipelines will first affect the normal development of oil and gas fields, causing huge economic losses, and also affect the supply of gas to residents, affecting their daily lives. Particularly serious is that the leaked natural gas can also cause malignant accidents such as fires and explosions, which directly threaten the safety of offshore platforms, ships, and personnel. However, there is still a lack of research on the impact of various parameters on the vertical direction of natural gas leakage and diffusion. Therefore, this paper used numerical simulation methods to study the diffusion and leakage of natural gas from subsea pipelines. The law of natural gas leakage and diffusion of submarine pipeline's and the effects of water depth at the leakage point, leakage aperture, pressure in the pipe, seawater flow velocity and other factors on natural gas leakage and diffusion of submarine pipeline were obtained. The main conclusions are as follows:

(1) The process of natural gas leakage and diffusion of a submarine pipeline is as follows: the leaked natural gas jet enters the seawater to form a gas mass, and the gas rises continuously under the action of pressure in the pipe and seawater buoyancy. The natural gas in the gas-transmission pipeline continuously enters the sea water, causing the

disturbance of the sea water, which makes the gas mass gradually form a mushroom shape. The gas masses break into smaller bubbles due to the interaction between the gas–liquid two phases, which continue to float and diffuse to the overflow surface.

(2) The time required for the leakage gas to diffuse and overflow the water surface increases with the increase of the water depth at the leakage port.

(3) The size of leakage aperture affects the amount of leakage, rising speed and the range of diffusion to the water surface, and is directly proportional to them.

(4) The greater the pressure in the pipe, the greater the initial momentum given to the leakage gas, which results in a faster rising speed and a shorter time required to diffuse to the water surface.

(5) The ocean current's velocity mainly affects the offset of leakage gas along the water-flow direction. The greater the ocean current's velocity, the farther the area where natural gas diffuses to the overflow sea surface is from the leakage port.

According to the law of natural gas leakage and diffusion of submarine pipelines and the influences of various factors on its leakage and diffusion, an efficient and reasonable emergency rescue plan can be formulated. A better plan for the development and utilization of marine natural gas resources can also be formulated so as to transform the blind and passive maintenance of submarine natural gas pipelines into predictive and active maintenance. This will effectively reduce casualties, reduce the incidence of safety accidents, reduce unnecessary economic losses, improve economic benefits and be conducive to the sustainable development of economy and environment.

Author Contributions: Conceptualization, M.Y.; software, M.Y.; formal analysis, Z.H.; investigation, X.W.; data curation, M.Y.; writing—original draft preparation, M.Y.; writing—review and editing, R.J. All authors have read and agreed to the published version of the manuscript.

Funding: This work was supported by the Science and Technology Department of Sichuan Provincial (2022NSFSC1154, 2021ZHCG0037, 2020ZHCG0005).

Institutional Review Board Statement: Not applicable.

Informed Consent Statement: Not applicable.

Data Availability Statement: Not applicable.

Conflicts of Interest: The author(s) declared no potential conflict of interest with respect to the research, authorship and/or publication of this article.

References

1. Offshore Energy Outlook 2018, International Energy Agency. Available online: https://www.iea.org/reports/offshore-energy-outlook-2018.2018 (accessed on 1 May 2018).
2. Li, X.; Khan, F.; Yang, M.; Chen, C.; Chen, G. Risk assessment of offshore fire accidents caused by subsea gas release. *Appl. Ocean Res.* **2021**, *115*, 102828. [CrossRef]
3. Yu, J.; Chen, H.; Yu, Y.; Yang, Z. A weakest t-norm based fuzzy fault tree approach for leakage risk assessment of submarine pipeline. *J. Loss Prev. Process Ind.* **2019**, *2019*, 103968.
4. Fang, N.; Chen, G.M.; Zhu, H.W.; Meng, H. Statistical analysis of leakage accidents of submarine pipeline. *Oil Gas Storage Transp.* **2014**, *33*, 99–103.
5. Olsen, J.E.; Skjetne, P. Current understanding of subsea gas release: A review. *Can. J. Chem. Eng.* **2015**, *94*, 209–219. [CrossRef]
6. An Undersea Natural Gas Leak Has Set Fire to the Sea in the Gulf of Mexico! Available online: https://www.163.com/dy/article/GE1861UJ051484S5.2021 (accessed on 4 July 2021).
7. Liu, C.; Li, Y.; Meng, L.; Wang, W.; Zhao, F.; Fu, J. Computational fluid dynamic simulation of pressure perturbations generation for gas pipelines leakage. *Comput. Fluids* **2015**, *119*, 213–223. [CrossRef]
8. Hou, Q. An FBG Strain Sensor-Based NPW Method for Natural Gas Pipeline Leakage Detection. *Math. Probl. Eng.* **2021**, *2021*, 5548503. [CrossRef]
9. Nadimi, N.; Javidan, R.; Layeghi, K. Efficient Detection of Underwater Natural Gas Pipeline Leak Based on Synthetic Aperture Sonar (SAS) Systems. *J. Mar. Sci. Eng.* **2021**, *9*, 1273. [CrossRef]

10. Kim, J.; Chae, M.; Han, J.; Park, S.; Lee, Y. The development of leak detection model in subsea gas pipeline using machine learning. *J. Nat. Gas Sci. Eng.* **2021**, *94*, 104134. [CrossRef]
11. Zhu, H.; Lin, P.; Pan, Q. A CFD (computational fluid dynamic) simulation for oil leakage from damaged submarine pipeline. *Energy* **2014**, *64*, 887–899. [CrossRef]
12. Yang, Z.; Yu, J.; Li, Z.; Chen, H.; Jiang, M.; Chen, X. Application of computational fluid dynamics simulation for submarine oil spill. *Acta Oceanol. Sin.* **2018**, *37*, 104–115. [CrossRef]
13. Zhu, H.; You, J.; Zhao, H. Underwater spreading and surface drifting of oil spilled from a submarine pipeline under the combined action of wave and current. *Appl. Ocean Res.* **2017**, *64*, 217–235. [CrossRef]
14. Jiang, M.; Yu, J.; Li, Z.; Zhong, W.; Wu, Z.; Yu, Y. Laboratory investigation into the oil diffusion from submarine pipeline under water flow. *Acta Oceanol. Sin.* **2018**, *37*, 96–103. [CrossRef]
15. Pham, L.H.H.P.; Rusli, R.; Shariff, A.M.; Khan, F. Dispersion of carbon dioxide bubble release from shallow subsea carbon dioxide storage to seawater. *Cont. Shelf Res.* **2020**, *196*, 104075. [CrossRef]
16. Gros, J.; Schmidt, M.; Dale, A.W.; Linke, P. Simulating and Quantifying Multiple Natural Subsea CO_2 Seeps at Panarea Island (Aeolian Islands, Italy) as a Proxy for Potential Leakage from Subseabed Carbon Storage Sites. *Environ. Sci. Technol.* **2019**, *53*, 10258–10268. [CrossRef]
17. Yapa, P.D.; Zheng, L.; Chen, F. A Model for Deepwater Oil/Gas Blowouts. *Mar. Pollut. Bull.* **2001**, *43*, 234–241. [CrossRef]
18. Yapa, P.D.; Chen, F. Behavior of Oil and Gas from Deepwater Blowouts. *J. Hydraul. Eng.* **2004**, *130*, 540–553. [CrossRef]
19. Dasanayaka, L.K.; Yapa, P.D. Role of plume dynamics phase in a deepwater oil and gas release model. *J. Hydro-Environ. Res.* **2009**, *2*, 243–253. [CrossRef]
20. De Freitas Tessarolo, L.; Innocentini, V.; Barreto, F.T.C.; Gonçalves, I.A. Formation dissolution and decomposition of gas hydrates in a numerical model for oil and gas from deepwater blowouts. *Mar. Pollut. Bull.* **2021**, *165*, 112103. [CrossRef]
21. Wang, B.; Socolofsky, S.A.; Lai, C.C.; Adams, E.E.; Boufadel, M.C. Behavior and dynamics of bubble breakup in gas pipeline leaks and accidental subsea oil well blowouts. *Mar. Pollut. Bull.* **2018**, *131*, 72–86. [CrossRef]
22. Zhu, S.-B.; Li, Z.-L.; Zhang, S.-M.; Liang, L.-L.; Zhang, H.-F. Natural gas pipeline valve leakage rate estimation via factor and cluster analysis of acoustic emissions. *Measurement* **2018**, *125*, 48–55. [CrossRef]
23. Malik, A.A.; Nasif, M.S.; Niazi, U.M.; Al-Waked, R. Numerical modelling of wind-influenced above sea gas dispersion and explosion risk analysis due to subsea gas release on multileveled offshore platform. *Appl. Ocean Res.* **2022**, *124*, 103208. [CrossRef]
24. Yapa, P.D.; Dasanayaka, L.K.; Bandara, U.C.; Nakata, K. A model to simulate the transport and fate of gas and hydrates released in deepwater. *J. Hydraul. Res.* **2010**, *48*, 559–572. [CrossRef]
25. Erik, O.J.; Tore, J.S.; Mark, R. CFD study of surface flow and gas dispersion from a subsea gas release. In Proceedings of the ASME 2014 33rd International Conference on Ocean, Offshore and Arctic Engineering, San Francisco, CA, USA, 8–13 June 2014.
26. Zhao, L.; Boufadel, M.C.; King, T.; Robinson, B.; Gao, F.; Socolofsky, S.A.; Lee, K. Droplet and bubble formation of combined oil and gas releases in subsea blowouts. *Mar. Pollut. Bull.* **2017**, *120*, 203–216. [CrossRef] [PubMed]
27. Li, X.; Chen, G.; Zhu, H.; Xu, C. Gas dispersion and deflagration above sea from subsea release and its impact on offshore platform. *Ocean Eng.* **2018**, *163*, 157–168. [CrossRef]
28. Li, X.; Chen, G.; Zhang, R.; Zhu, H.; Fu, J. Simulation and assessment of underwater gas release and dispersion from subsea gas pipelines leak. *Process Saf. Environ. Prot.* **2018**, *119*, S0957582018305548.
29. Li, X.; Chen, G.; Khan, F. Analysis of underwater gas release and dispersion behavior to assess subsea safety risk. *J. Hazard. Mater.* **2019**, *367*, 676–685. [CrossRef]
30. Wu, K.; Cunningham, S.; Sivandran, S.; Green, J. Modelling subsea gas releases and resulting gas plumes using Computational Fluid Dynamics. *J. Loss Prev. Process. Ind.* **2017**, *49*, 411–417. [CrossRef]
31. Hou, Q.; Yang, D.; Li, X.; Xiao, G.; Ho, S.C.M. Modified Leakage Rate Calculation Models of Natural Gas Pipelines. *Math. Probl. Eng.* **2020**, *2020*, 6673107. [CrossRef]
32. Chopkap Noume, H.; Bomba, V.; Obounou, M.; Ekobena Fouda, H.P.; Sapnken, F.E. CFD study of a non-premixed turbulent flame using OpenFOAM: Effect of chemical mechanisms and turbulence models. *J. Energy Resour. Technol.* **2021**, *143*, 1–14.
33. Pourhoseini, S.H.; Ramezani-Aval, H. Effect of Application of Electric Force to Diesel Fuel Droplets Charged Through Millikan Oil-Drop Experiment on Physical and Thermal Characteristics of Flame. *J. Energy Resour. Technol.* **2021**, *144*, 062306. [CrossRef]
34. Wu, H.; Wang, B.; DiMarco, S.F.; Tan, L. Impact of bubble size on turbulent statistics in bubble plumes in unstratified quiescent water. *Int. J. Multiph. Flow* **2021**, *141*, 103692. [CrossRef]
35. Chen, J.; Tong, S.; Han, T.; Song, H.; Pinheiro, L.; Xu, H.; Azevedo, L.; Duan, M.; Liu, B. Modelling and detection of submarine bubble plumes using seismic oceanography. *J. Mar. Syst.* **2020**, *209*, 103375. [CrossRef]
36. Abousabae, M.; Amano, R.S. Air Flow Acceleration Effect on Water Droplet Flow Behavior in Solid Rocket Motor. *J. Energy Resour. Technol.* **2022**, *144*, 082305. [CrossRef]
37. Ziółkowski, P.; Szewczuk-Krypa, N.; Butterweck, A.; Stajnke, M.; Głuch, S.; Drosińska-Komor, M.; Milewska, A.; Głuch, J. Comprehensive Thermodynamic Analysis of Steam Storage in a Steam Cycle in a Different Regime of Work: A Zero-Dimensional and Three-Dimensional Approach. *J. Energy Resour. Technol.* **2022**, *144*, 050905. [CrossRef]

38. Kolla, S.S.; Mohan, R.S.; Shoham, O. Numerical Analysis of Flow Behavior in Gas–Liquid Cylindrical Cyclone (GLCC©) Separators With Inlet Design Modifications. *J. Energy Resour. Technol.* **2021**, *143*, 093005. [CrossRef]
39. Wilkening, H.; Baraldi, D. CFD modelling of accidental hydrogen release from pipelines. *Int. J. Hydrogen Energy* **2007**, *32*, 2206–2215. [CrossRef]
40. Engebretsen, T.; Northug, T.; Sjøen, K.; Fanneløp, T.K. Surface Flow and Gas Dispersion from a Subsea Release of Natural Gas. In Proceedings of the Seventh International Offshore and Polar Engineering Conference, Honolulu, HI, USA, 25–30 May 1997; ISOPE-I-97-086.